

ON THE INFLUENCE OF MODEL PARAMETRIZATION IN ELASTIC FULL WAVEFORM TOMOGRAPHY

D. Köhn, D. De Nil, A. Kurzmann, A. Przebindowska, N. Nguyen, and T. Bohlen

email: *daniel.koehn@geophysik.tu-freiberg.de*

keywords: *reflection seismic imaging, elastic waveform inversion, full wavefield, parametrization*

ABSTRACT

With the increasing performance of parallel supercomputers full waveform tomography (FWT) approaches can reduce the misfit between recorded and modelled data, to deduce a very detailed physical model of the underground. In recent years acoustic waveform tomography became a very popular tool to image the underground structures. However, acoustic waveform inversion has the disadvantage, that only P waves can be inverted. It can not invert for S-waves or surface waves. Here we will investigate the influence of parametrization on resolution and ambiguity using our elastic parallel time domain FWT code with two synthetic model examples. Even though the problem is highly nonlinear and ill conditioned the elastic FWT is able to resolve very detailed images of all three elastic model parameters.

INTRODUCTION

Full waveform tomography (FWT) is a state of the art imaging concept, which requires a massive amount of computer resources. Therefore the first applications of FWT for moderate 2D problems were undertaken in the late 1990s (Pratt (1999), Pratt and Shipp (1999)) for the acoustic case. The application of elastic FWT is even more complicated, because 3 coupled elastic parameters have to be optimized at the same time. In this paper we give a short overview of the first results we achieved with the elastic time domain FWT code DENISE (subwavelength DEtail resolving Nonlinear Iterative SEismic inversion). As the name already states the FWT can only image structures at or below the seismic wavelength. The long wavelength part of the model has to be estimated by other methods like first arrival tomography. In this paper we investigate the influence of different model parametrizations on the FWT result.

THEORETICAL BACKGROUND

The aim of full waveform tomography is to minimize the data residuals $\delta \mathbf{u} = \mathbf{d}^{\text{mod}} - \mathbf{d}^{\text{obs}}$ between the modelled data \mathbf{d}^{mod} and the field data \mathbf{d}^{obs} . The misfit can be measured by the residual energy:

$$E = \frac{1}{2} \delta \mathbf{u}^T \delta \mathbf{u}. \quad (1)$$

The residual energy can be minimized by updating the model parameters \mathbf{m}_n at iteration step n using a steepest-descent gradient method:

$$\mathbf{m}_{n+1} = \mathbf{m}_n - \mu_n \mathbf{P} \delta \mathbf{m}_n, \quad (2)$$

where $\delta \mathbf{m}$ denotes the steepest-descent direction of the objective function and μ_n the step length. To increase the convergence speed of the FWT code the application of a preconditioning operator \mathbf{P} is recommended.

According to Mora (1987) the gradients for the Lamé parameters λ , μ and the density ρ can be expressed as:

$$\begin{aligned}\delta\lambda &= -\sum_S \int dt \left(\frac{\partial u_x}{\partial x} + \frac{\partial u_y}{\partial y} \right) \left(\frac{\partial \Psi_x}{\partial x} + \frac{\partial \Psi_y}{\partial y} \right), \\ \delta\mu &= -2 \sum_S \int dt \left(\frac{\partial u_x}{\partial y} + \frac{\partial u_y}{\partial x} \right) \left(\frac{\partial \Psi_x}{\partial y} + \frac{\partial \Psi_y}{\partial x} \right) + \left(\frac{\partial u_x}{\partial x} \frac{\partial \Psi_x}{\partial x} - \frac{\partial u_y}{\partial y} \frac{\partial \Psi_y}{\partial y} \right), \\ \delta\rho &= -\sum_S \int dt \left(\frac{\partial u_x}{\partial t} \frac{\partial \Psi_x}{\partial t} + \frac{\partial u_y}{\partial t} \frac{\partial \Psi_y}{\partial t} \right),\end{aligned}\quad (3)$$

where u_i denotes the i th component of the forward displacement wavefield, while

$$\Psi_j(\mathbf{x}, t) = -\sum_R G_{ij}(\mathbf{x}, -t; \mathbf{x}_R, 0) * \delta u_i(\mathbf{x}_R, t). \quad (4)$$

is a wavefield generated by propagating the residual data δu_i from the receiver positions backwards in time into the medium. G_{ij} denotes the Green's function solution of the elastic wave equation.

The gradients for other material parameters m_{new} can be calculated by applying the chain rule on the Frechét kernel in the adjoint problem:

$$\delta \mathbf{m}_{\text{new}} = \sum_S \int dt \sum_R \left[\frac{\partial \mathbf{d}}{\partial \mathbf{m}} \frac{\partial \mathbf{m}}{\partial m_{\text{new}}} \right]^* \delta u_i \quad (5)$$

Using the relationships between P-wave velocity V_p , S-wave velocity V_s , the Lamé parameters λ , μ and density ρ :

$$V_p = \sqrt{\frac{\lambda + 2\mu}{\rho}}, \quad V_s = \sqrt{\frac{\mu}{\rho}} \quad (6)$$

or

$$\lambda = \rho V_p^2 - 2\rho V_s^2, \quad \mu = \rho V_s^2 \quad (7)$$

the gradient for V_p can be written as:

$$\begin{aligned}\delta V_p &= \sum_S \int dt \sum_R \left[\frac{\partial \mathbf{d}}{\partial \lambda} \frac{\partial \lambda}{\partial V_p} + \frac{\partial \mathbf{d}}{\partial \mu} \frac{\partial \mu}{\partial V_p} + \frac{\partial \mathbf{d}}{\partial \rho} \frac{\partial \rho}{\partial V_p} \right]^* \delta u_i \\ &= \sum_S \int dt \sum_R \left[\frac{\partial \mathbf{d}}{\partial \lambda} 2\rho V_p \right]^* \delta u_i \\ &= 2\rho V_p \sum_S \int dt \sum_R \left[\frac{\partial \mathbf{d}}{\partial \lambda} \right]^* \delta u_i \\ &= 2\rho V_p \delta \lambda\end{aligned}\quad (8)$$

The gradients for V_s and ρ are calculated in a similar way, so the gradients in terms of seismic velocities can be written as:

$$\begin{aligned}\delta V_p &= 2\rho V_p \delta \lambda, \\ \delta V_s &= -4\rho V_s \delta \lambda + 2\rho V_s \delta \mu, \\ \delta \rho_{\text{vel}} &= (V_p^2 - 2V_s^2) \delta \lambda + V_s^2 \delta \mu + \delta \rho\end{aligned}\quad (9)$$

In summary one iteration step of the elastic FWT algorithm consists of the following steps:

1. For each shot S solve the elastic wave equation for the actual model \mathbf{m}_n to generate a synthetic seismograms \mathbf{d}^{mod} and the wavefield $\mathbf{u}(\mathbf{x}, t)$.
2. Calculate the residual seismograms $\delta\mathbf{u} = \mathbf{d}^{\text{mod}} - \mathbf{d}^{\text{obs}}$.
3. Generate the wavefield $\Psi(\mathbf{x}, t)$ by backpropagating the residuals from the receiver positions R .
4. Calculate the optimum perturbations $\delta\mathbf{m}$ of each material parameter according to (3) or (5).
5. Apply an appropriate preconditioning operator P .
6. Estimate the step length μ_n by a line search.
7. Update the material parameters using the gradient method $\mathbf{m}_{n+1} = \mathbf{m}_n - \mu_n P \delta\mathbf{m}$.

In our FWT code the forward problem and backpropagation of the residual wavefield are solved using a parallel time domain finite difference code (Bohlen (2002)).

THE CTS TEST PROBLEM

To investigate the influence of different model parametrizations we build two elastic models for the parameter sets $\mathbf{m}_1 = [\lambda, \mu, \rho]$ and $\mathbf{m}_2 = [V_p, V_s, \rho]$ (Fig. 1). The models consist of a free surface at the top, an elastic layer and a half space. Seismic body waves are traveling from the sources at the surface and are reflected back to the surface at the interface between the layer and half space. Embedded in the layer are different geometrical bodies, which are disturbing the wavefield of the reflected waves. These geometrical bodies consist of

1. 7 crosses indicating perturbations of the Lamé parameter λ and the P-wave velocity V_p .
2. 8 triangles indicating perturbations of the Lamé parameter μ and the S-wave velocity V_s .
3. 6 squares indicating perturbations of the density ρ .

Due to the different geometrical structures we call this model Cross-Triangle-Squares (CTS) model. The geometrical bodies are located at different non overlapping places. This does not represent a realistic geological situation, but it is an effective way to demonstrate the resolution and ambiguity of the FWT result when using different elastic parametrizations. The S-wave velocity V_s and density ρ for the different geometrical structures are calculated from the P-wave velocity V_p of the crosses using the following relationships

$$\begin{aligned} V_s &= V_p / \sqrt{3}, \\ \rho &= 0.31 * 1000.0 * V_p^{1/4}. \end{aligned} \tag{10}$$

The corresponding models for the Lamé parameters are calculated using the relationships in Eq. (7), but without mixing the structural models. Therefore the resulting models for seismic velocities and Lamé parameters are not equivalent and the resulting wavefields are different, which can be easily seen by comparing the seismic sections for the different parametrizations in Fig. 3 (c). The acquisition geometry consists of 100 explosive sources 40 m below the free surface. The source signature is a Ricker wavelet with a centre frequency of 5 Hz and a maximum frequency of 10 Hz. The elastic wavefield is recorded by 400 two component receivers in 40 m depth. Using an 8th order spatial FD operator for the forward modelling and backpropagation of the wavefield the model can be discretized with 500×150 gridpoints in x- and y-direction with a spatial gridpoint distance of 20.0 m. The time is discretized using $DT = 2.7$ ms, thus for a recording time of $T = 6.0$ s 2222 time steps are required. Synthetic multicomponent datasets are calculated for the CTS model and inverted using a starting model with the correct elastic material parameters for the layer and the half space but without the geometrical structures. In Fig. 2 the inversion results are shown using the Lamé parameters and the seismic velocities as elastic inversion parameters. In both cases the elastic

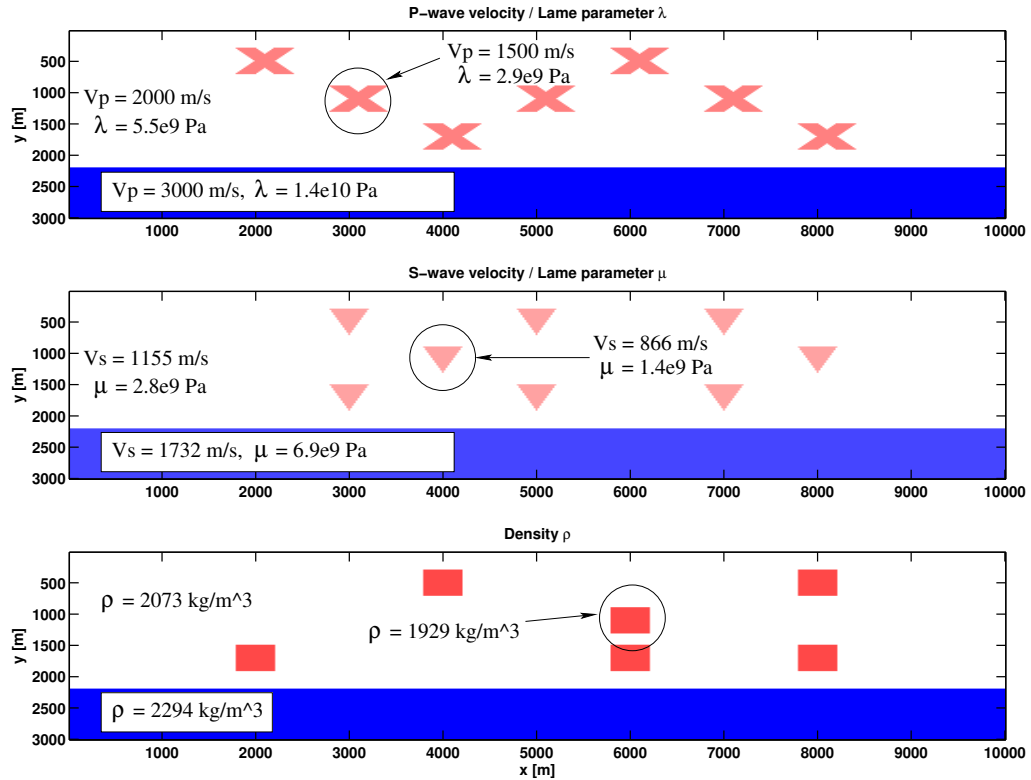


Figure 1: The Cross-Triangle-Squares test problem for the parameter sets $\mathbf{m}_1 = [\lambda, \mu, \rho]$ and $\mathbf{m}_2 = [V_p, V_s, \rho]$.

parameters could be reconstructed very well without any ambiguity. The Lamé parameter λ shows a little bit more artefacts than the P-wave velocity V_p , but the results are still quite similar in terms of resolution. Surprisingly the choice of parameters has a huge impact on the density results. Using Lamé parameters the squares of the density model could be recovered very well, but they are disturbed by extremely large triangular shaped μ artefacts which would hide the true density result in a geological more realistic setting. When using seismic velocities as model parameters a stronger ambiguity is present, the crosses of the V_p model and the triangles of the V_s model are partly interpreted as density information, but they have the same magnitude as the true density model. In Fig. 3 the seismic sections of shot 50 are plotted for the starting model (a), the inversion result (b) the true model (c), the initial residuals (d), the final residuals (e) and the evolution of the residual energy (f) using the different parametrizations. The fit of the phases and amplitudes is very good in both cases. Even though the final residuals are a bit larger in case of the seismic velocities (Fig. 3 (e)).

A COMPLEX GEOLOGICAL TEST PROBLEM - THE ELASTIC MARMOUSI MODEL

A widely used test problem for seismic imaging techniques is the elastic Marmousi-II model (Fig. 4, Martin et al. (2006)). The model consists of horizontal layers near the boundaries, while steep thrust faults are disturbing the layers. The deeper parts of the model consist of salt and reef structures. The thrust fault system and the reef structures are not easy to resolve by conventional first arrival tomography, so it is an ideal test model for the FWT. Due to computational restrictions the original Marmousi-II model could not be used, because the very low S-wave velocities in the sediments would require a too small spatial sampling of the model. Therefore new S-wave velocities are calculated using scaling relation (10).

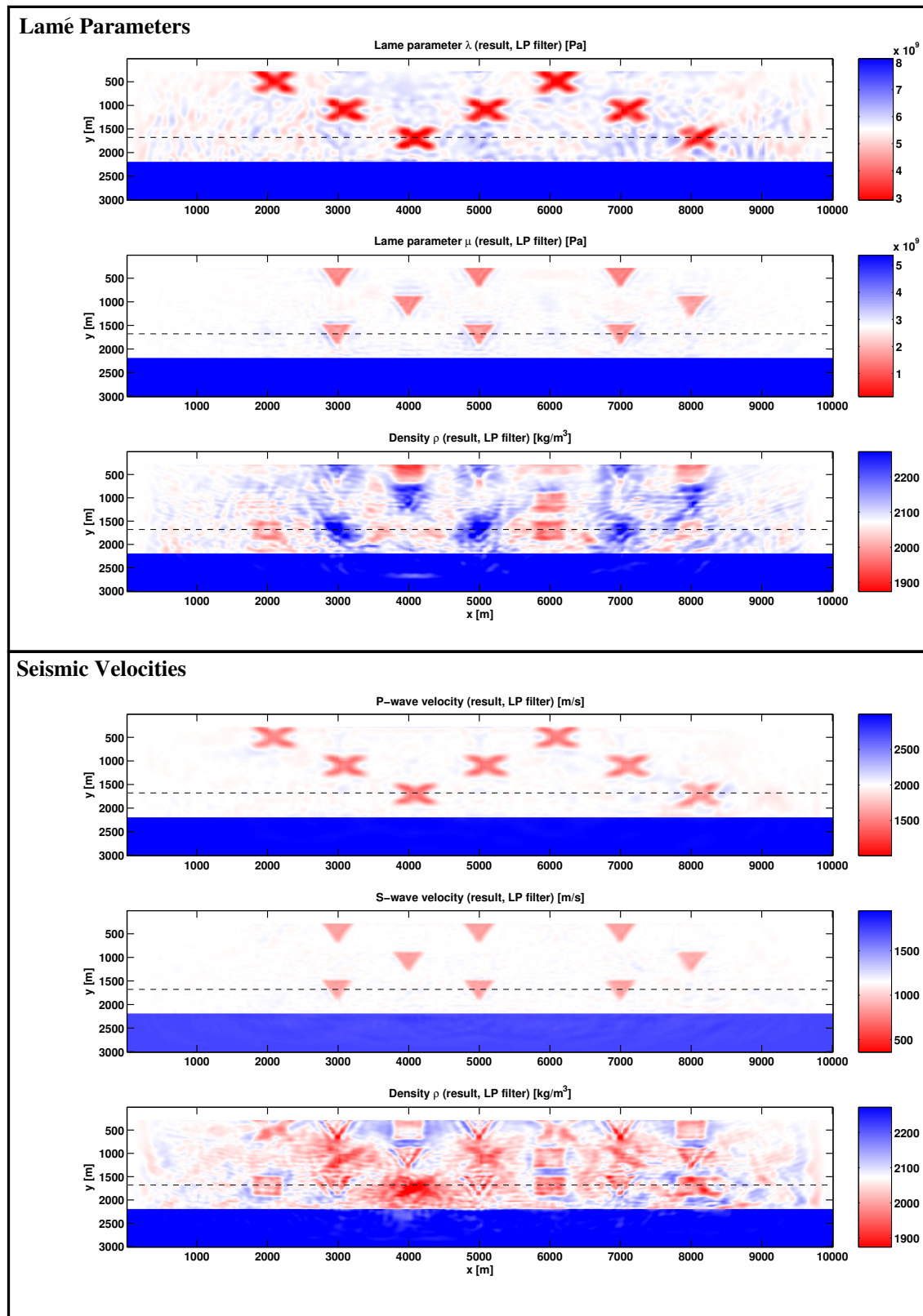


Figure 2: Results of the FWT for the Cross-Triangle-Squares model using Lamé parameters (top) and seismic velocities (bottom) as inversion parameters.

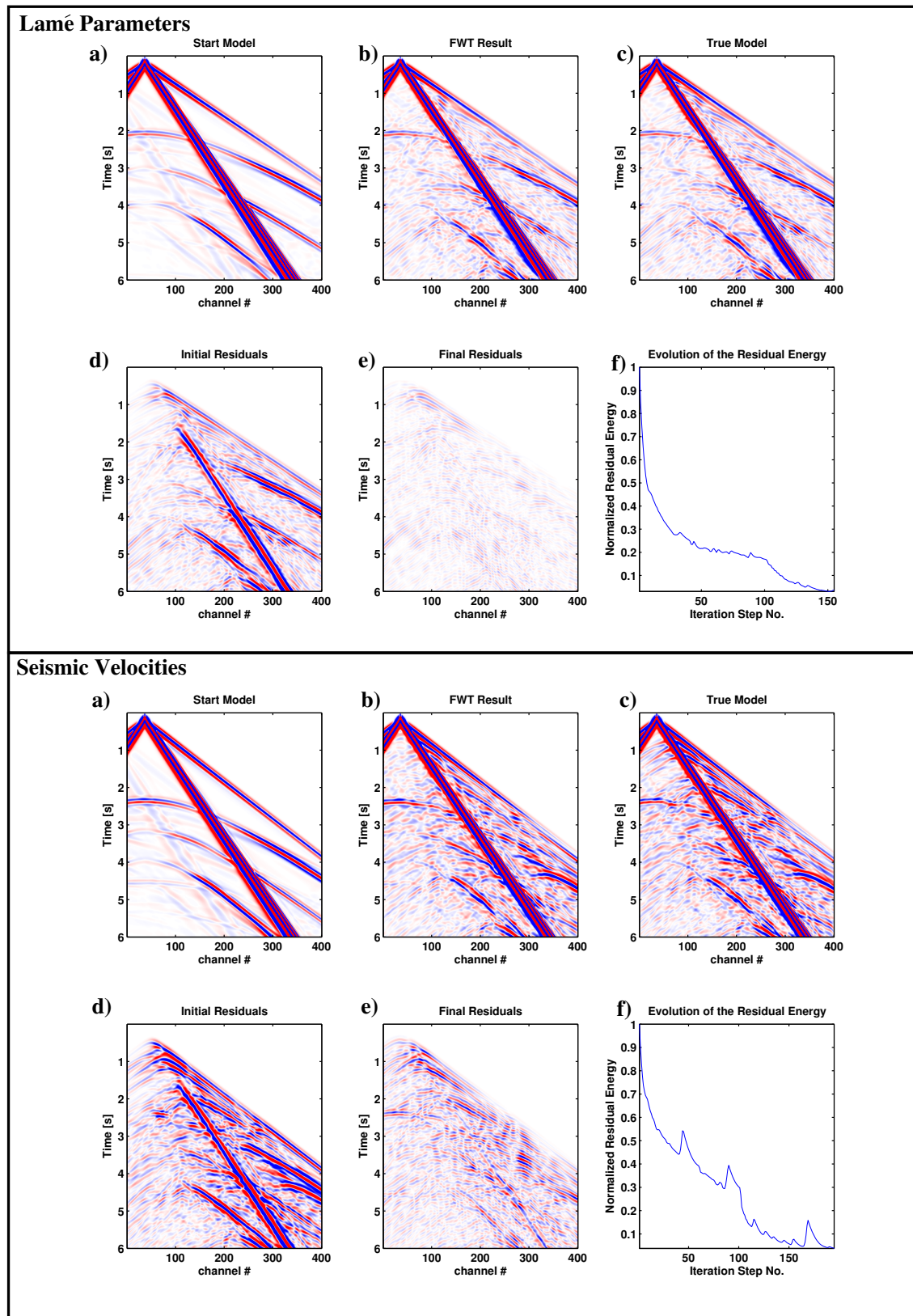


Figure 3: Seismic sections for the Cross-Triangle-Squares model using Lamé parameters (top) and seismic velocities (bottom). (a) starting model, (b) FWT result, (c) true model, (d) initial residuals, (e) final residuals and (f) evolution of the residual energy.

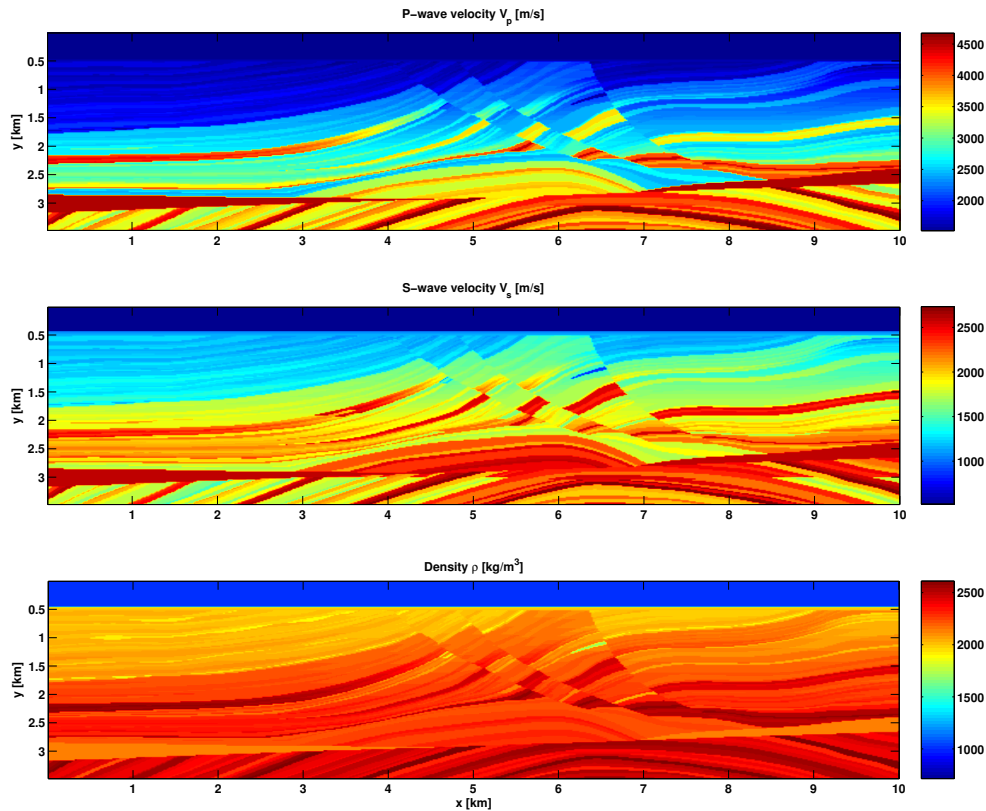


Figure 4: The Marmousi-II model.

The acquisition geometry consists of a streamer towed 40 m below the free surface with 400 two component receivers in a 500 m thick water layer. The synthetic dataset consists of 100 airgun shots. The source signature is a 10 Hz Ricker wavelet. Using an 8th order spatial FD operator the model can be discretized with 500×174 gridpoints in x- and y-direction with a spatial gridpoint distance of 20.0 m. The time is discretized using $DT = 2.7$ ms, thus for a recording time of $T = 6.0$ s 2222 time steps are needed.

Due to the results of the last section, we choose the seismic velocities as model parameters for the inversion. The starting model (Fig. 5) is a median filtered version of the true model. To achieve a smooth transition from the long wavelength starting model to the inversion result with short wavelength structures the application of a frequency filter with variable bandwidth on the data residuals $\delta \mathbf{u}$ is vital, to avoid the convergence into a local minimum. In this case the inversion is separated in two parts. In part I only frequencies below 10 Hz are inverted, while in part II the full spectral content up to 20 Hz is inverted.

The inversion results after 350 iterations are shown in Fig. 6. The results contain a lot of small details and fine layers which are completely absent in the starting model. The thrust faults and the reef structures in the deeper part of the model are imaged very well. It is quite surprising, that the shear wave velocity model could also be resolved very well, even though only streamer data and therefore mainly P-wave information is used. Even the density, a parameter which can be hardly estimated from seismic data, could be recovered from the seismic wavefield. In Fig. 7 the seismic sections of shot 50 are plotted for the starting model (a), the inversion result (b) the true model (c), the initial residuals (d), the final residuals (e) and the evolution of the residual energy (f). Notice the good fit of the first arrivals for the starting model, but the lack of small details beyond the first arrivals. Only the direct wave, the reflection from the ocean bottom and a few multiples are present. The inversion result fits the phases and amplitudes of the later small scale arrivals.

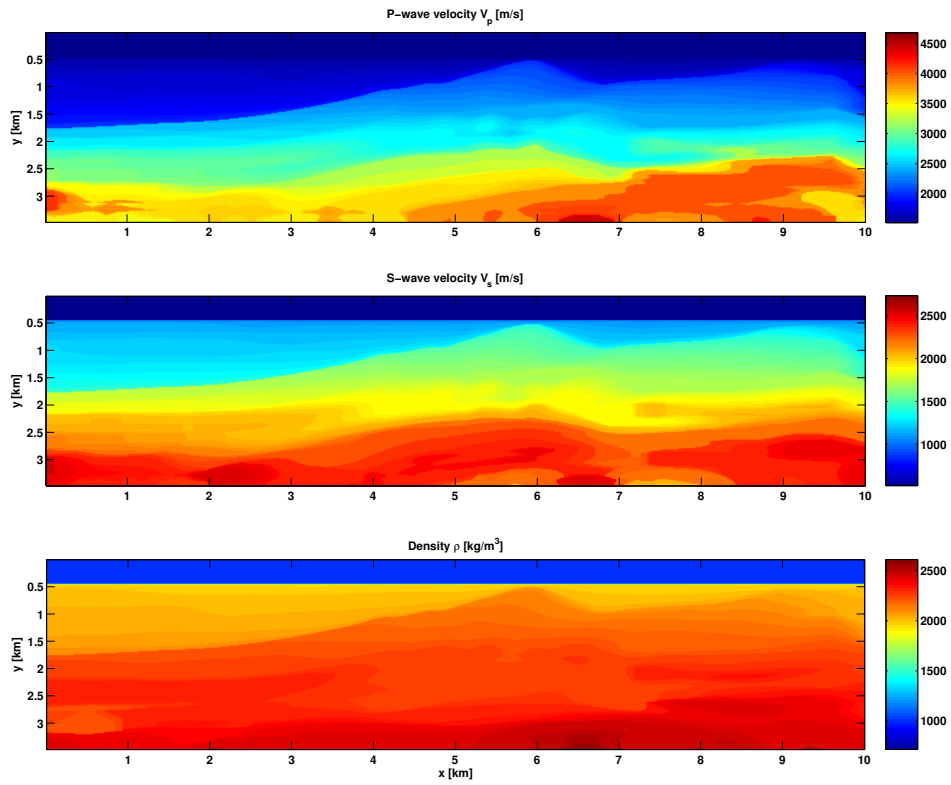


Figure 5: Starting models for the Marmousi-II model.

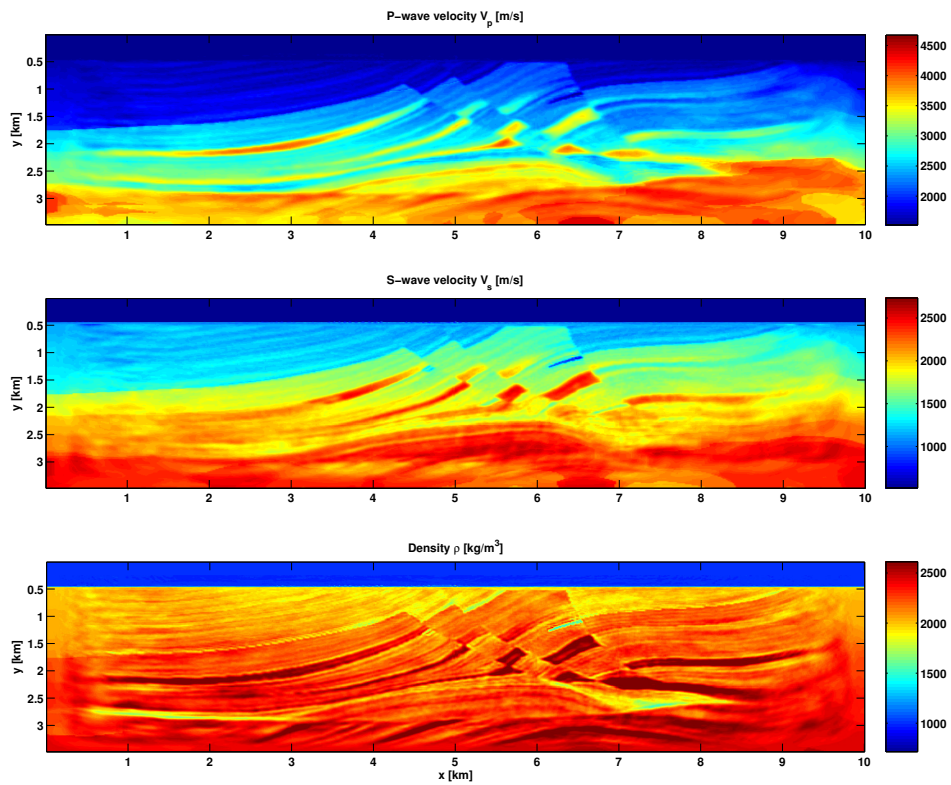


Figure 6: Results of the elastic FWT for the Marmousi-II model.

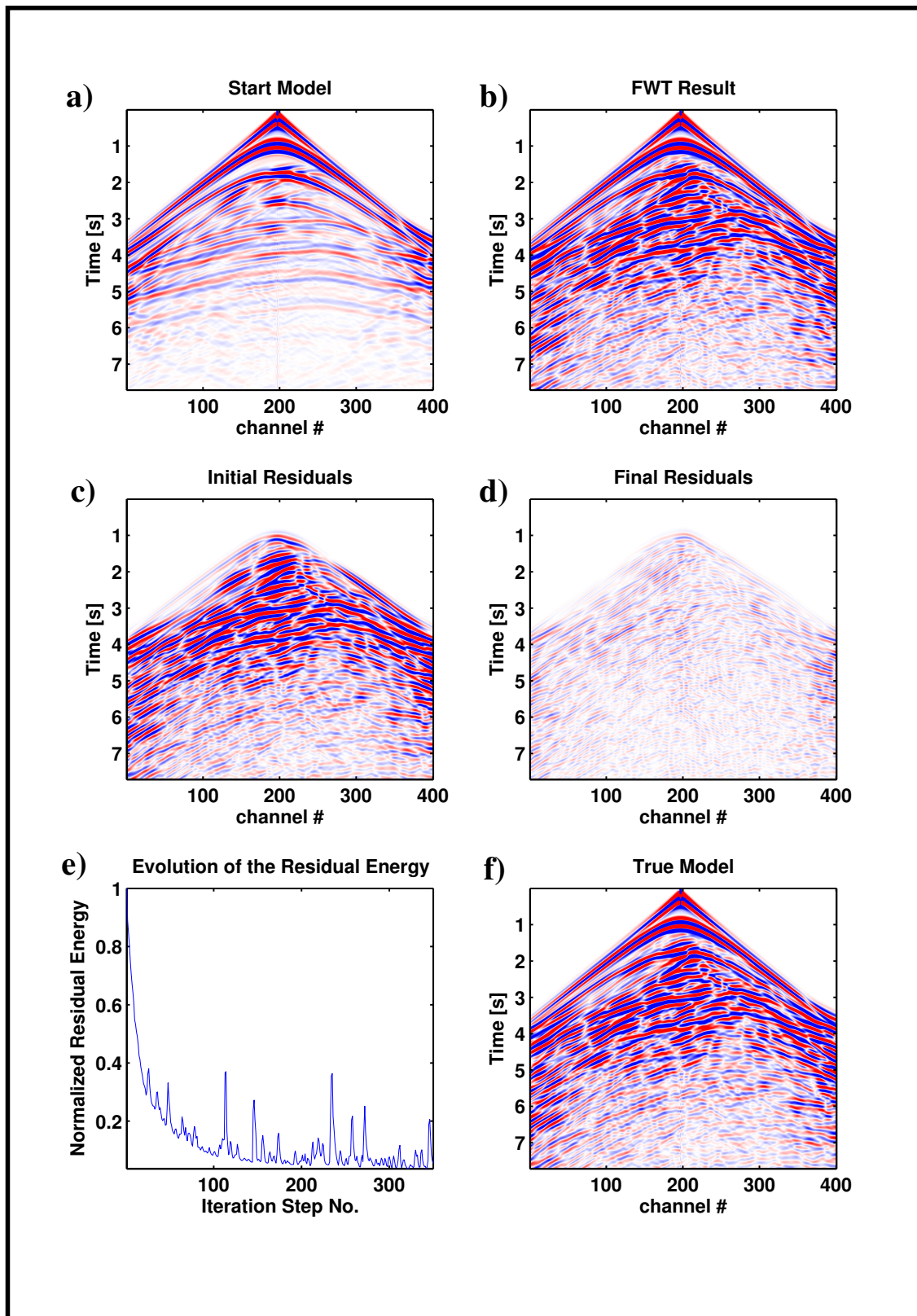


Figure 7: Seismic sections for the Marmousi-II model. (a) starting model, (b) FWT result, (c) initial residuals, (d) final residuals, (e) true model and (f) evolution of the residual energy.

CONCLUSIONS AND OUTLOOK

In this paper we have shown the potential of elastic FWT for imaging structures which are on the same scale or smaller than the seismic wavelength. The success of FWT highly depends on the choice of model parameters. For a successful joint inversion of all three elastic parameters it is essential to choose the seismic velocities as model parameters. This could be demonstrated using the CTS model for different parametrizations. The Lamé parameters produce strong density artefacts, while these artefacts are absent when using seismic velocities. The choice of the seismic velocities also improves the image quality when using a geological more realistic model, like the elastic Marmousi-II model. First tests with OBC data already looked very good, but even with streamer data the resolution of the elastic model is very impressive.

REFERENCES

- Bohlen, T. (2002). Parallel 3-D viscoelastic finite-difference seismic modelling. *Computers & Geosciences*, 28(8):887–899.
- Martin, G., Wiley, R., and Marfurt, K. (2006). Marmousi2 - An elastic upgrade for Marmousi. *The Leading Edge*, 25:156–166.
- Mora, P. (1987). Nonlinear two-dimensional elastic inversion of multioffset seismic data. *Geophysics*, 52:1211 – 1228.
- Pratt, R. (1999). Seismic waveform inversion in the frequency domain, Part 1: Theory and verification in a physical scale model. *Geophysics*, 64:888–901.
- Pratt, R. and Shipp, R. (1999). Seismic waveform inversion in the frequency domain, Part 2: Fault delineation in sediments using crosshole data. *Geophysics*, 64:902–914.